Numerical study of the stability of double fingers with the phase-field model

Seiji Tokunaga and Hidetsugu Sakaguchi
Department of Applied Science for Electronics and Materials, Interdisciplinary of Engineering Sciences, Kyushu University, Kasuga, Fukuoka 816-8580, Japan

(Received 6 June 2003; revised manuscript received 8 December 2003; published 27 July 2004)

Doublon is one of the typical patterns found in crystal growth. It is a bound state of two fingerlike patterns. In this paper, we obtain a phase diagram for doublons with numerical simulations of the phase-field model. Numerical simulations are performed in a channel. Two small seeds of crystal with different sizes are set on the left side of the channel as an initial condition, in order to find whether the two fingers grow into a doublon or one finger overcomes the other owing to mutual competition. It is confirmed that a stable doublon is formed when the undercooling is large and the anisotropy is weak. Furthermore, we find a doublon with oscillating groove in a certain parameter range. We investigate more carefully the transition between the doublon and the dendrite by changing the anisotropy parameters stepwise, and show that the difference of the tip velocities of the doublon and the dendrite increases continuously from zero at a critical value of anisotropy.

DOI: 10.1103/PhysRevE.70.011607 PACS number(s): 68.08.−p, 82.40.Ck, 05.45.−a

I. INTRODUCTION

Crystal growth has been intensively studied as a problem of pattern formations far from equilibrium [1–3]. Many fascinating patterns such as dendrites have been studied in experiments of crystal growth [4–6] and computer simulations [7–9]. Recently, the phase-field model is one of the popular methods of computer simulations for crystal growth [10–13].

Doublon is one of the typical growth patterns in diffusion fields. It takes a form composed of a pair of fingers. There is a narrow groove between the two fingers. It has the mirror symmetry with respect to the center of the groove. This doublon structure was first predicted by Ben Amar and Brener as an asymmetric dendrite along the sidewall [14]. They showed analytically that the growth velocity of doublons is proportional to the ninth power of the undercooling, which is quite different from the normal dendrite. The doublons were found in several experiments. Jamgotchian *et al.* and Akamatsu *et al.* found some doublons in experiments of directional solidification [15]. They confirmed that the doublons appear under the condition of low anisotropy and high undercooling. Furthermore, they discovered that the width of groove is in inverse proportion to the undercooling. Losert *et al.* investigated the formation and the stability of doublons, changing the wavelength and strength of fluctuations in experiments of directional solidification and numerical simulations of the phase-field model [16]. The doublons were also found in an experiment of a drying water film by Lipson's group [17]. Doublons are considered to exist in a parameter region where the dense branching morphology (DBM) appears. Ihle, Müller-Krumbhaar and Brener discussed qualitatively the stability region of doublons in a parameter space of surface tension anisotropy and undercooling [18,19]. Brener *et al.* first observed the doublon structure with a numerical simulation in a channel [20] and a more careful analysis of the transition from the dendrite to the doublon in a channel was done by Kupferman *et al.* [21].

A phase-field model is a useful model for numerical simulation of growth patterns. It has a form of coupled equations of the Ginzburg-Landau equation and the diffusion equation. For melt growth, the Ginzburg-Landau equation represents the dynamics of phase transition from liquid to solid. The diffusion equation expresses heat conduction of the latent heat released at the growing interface. An order parameter p changes smoothly at an interface of the liquid and the solid. An appealing point of the phase-field model is that we need not solve the difficult Stefan problem with moving boundary conditions at the interface. By the improvement of the phase-field model by Karma and Rappel, it became possible to simulate crystal growth without the kinetic effect [11].

In this paper, we investigate the stability of doublons in a space of anisotropy parameters and undercooling. To find the stable region, we perform numerical simulations of the phase-field model in a channel. Two seeds of crystals with different sizes are initially set on the left side of the channel. They grow into two fingers and interact with each other through the diffusion field. If one finger wins and the tip positions of the two fingers separate away, we judge that a doublon has not been formed at the parameter. On the other hand, if the other finger catches up and the tip positions approach, we judge that a doublon is stable at the parameter. We use a channel system to focus on the competitive time evolution of two fingers. In contrast, if we use a large square box for the simulation, many fingers are created naturally and it will become difficult to judge the formation of doublons. A channel system is simpler in this sense, however, the effects of the sidewalls of the channel are not negligible especially for small undercooling, and it makes the transition between the dendrite and the doublon more complicated as shown by Kupferman *et al.* [21].

In Sec. II, we introduce our model equation and the numerical method. In Sec. III, we show the numerical results. In Sec. III A, we study the tip velocity of doublons in case of no anisotropy. The growing velocity is in proportional to the ninth power of the undercooling. In Sec. III B, we show the results of simulations in case of no kinetic effect, and in Sec. III C, involving kinetic effect.

In Sec. IV A, we study the transition between the doublon and the dendrite, changing the anisotropy parameters step-

wise, and in Sec. IV B we study groove oscillation of doublons more in detail.

II. MODEL EQUATIONS

The phase-field model is expressed as

$$\tau(\theta)\partial_t p = \{p - \lambda u(1-p^2)\}(1-p^2) + \partial_x\{W(\theta)^2\partial_x p - W(\theta)W'(\theta)\partial_y p\} + \partial_y\{W(\theta)^2\partial_y p + W(\theta)W'(\theta)\partial_x p\}, \quad (1)$$

$$\partial_t u = D\nabla^2 u + \partial_t p/2, \quad (2)$$

where p is an order parameter, $p=1$ and -1 correspond to solid and liquid phase, respectively, λ is a dimensionless parameter that controls the coupling strength between the order parameter and the diffusion field, $\tau(\theta)$ is an anisotropic time constant, $W(\theta)^2$ is an anisotropic diffusion constant and $W'(\theta)=dW/d\theta$. The variable u represents the dimensionless temperature: $u=(T-T_M)/(L/C_p)$ where T, T_M, L, and C_p are, respectively, the temperature, the melting temperature, the latent heat, and the specific heat at constant pressure. The diffusion constant for u is denoted by D. The term $\partial_t p/2$ in Eq. (2) expresses the release of latent heat at the interface. The angle $\theta \equiv \arctan(\partial_y p/\partial_x p)$ represents the direction normal to the contour of constant p. The fourfold rotational symmetry is assumed for the two types of anisotropies:

$$W(\theta) = 1 + e_s\cos(4\theta), \quad (3)$$

$$\tau(\theta) = W(\theta)\{1 + e_k\cos(4\theta)\}, \quad (4)$$

where the parameters e_s and e_k denote strength of surface tension anisotropy and that of kinetic anisotropy respectively. Constants parts of W and τ are assumed to be 1 in Eqs. (3) and (4). They determine the spatial and time scales of the order parameter. In this paper, we express length and time with these units. Karma and Rappel derived the sharp-interface limit of the phase-field model as

$$\partial_t u = D\nabla^2 u, \quad (5)$$

$$u_i = -d_0(\theta)\kappa - \beta(\theta)v_n. \quad (6)$$

Equation (5) is the diffusion equation for u and Eq. (6) is the generalized Gibbs-Thomson condition, respectively, where $d_0(\theta)$, κ, $\beta(\theta)$ and v_n denote respectively the anisotropic capillary length, the interface curvature, the anisotropic kinetic coefficient and the normal interface velocity. These parameters can be expressed using $W(\theta)$ and $\tau(\theta)$ as

$$d_0(\theta) = \frac{I}{\lambda J}\{W(\theta) + W''(\theta)\}, \quad (7)$$

$$\beta(\theta) = \frac{I}{\lambda J}\frac{\tau(\theta)}{W(\theta)}\left[1 - \lambda\frac{W^2(\theta)}{2D\tau(\theta)}\frac{K+JF}{I}\right], \quad (8)$$

where $I=2\sqrt{2}/3$, $J=16/15$, $F=\sqrt{2}\ln 2$, and $K=0.13604$. If the relation $\tau(\theta)=W(\theta)^2$ is assumed and the parameter λ is chosen as $\lambda=(2ID)/(K+JF)$, the anisotropic kinetic coefficient $\beta(\theta)$ becomes zero, that is, the kinetic effect becomes negligible, and then the capillary length is expressed as $d_0(\theta)=d_0[1-15e_s\cos(4\theta)]$, where $d_0=I/(\lambda J)\approx 0.2769$. If the parameter λ is chosen such as $\lambda=(1.8ID)/(K+JF)$, the anisotropic coefficients $d_0(\theta)$ and $\beta(\theta)$ are expressed as $d_0(\theta)=d_0[1-15e_s\cos(4\theta)]$ and $\beta(\theta)=d_0[0.1+(e_k-0.9e_s)\cos 4\theta]$ where $d_0=I/(\lambda J)\approx 0.3077$. We use these two parameters as typical cases without the kinetic effect and with kinetic effect. We have performed numerical simulations of the phase-field model (1), (2) with the finite difference method of gridsize $\Delta x=0.4$ and timestep $\Delta t=0.015$. The simulations were performed in a channel (a rectangular box) of size $L_x\times L_y=480\times 192$ (Sec. III) and 480×200 (Sec. IV). Kupferman *et al.* studied an asymmetric dendrite (half of the doublon) in a channel [21] by solving numerically an integro-differential equation for the interface. The channel width L_y of their system is 2, the capillary length d_0 is 0.01, and the ratio is $L_y/d_0=200$. On the other hand, our system has a ratio $L_y/d_0\approx 200/0.2769=722$, although two fingers grow in our system. The diffusion constant is fixed to be $D=2$. The anisotropy parameters e_s and e_k are changed from 0 to 0.06. On the other hand, Kupferman *et al.* studied the transitions between the dendrite and the doublon at three parameters $e_s=0$,0.006 and 0.00667. The initial conditions are $p(x,y,t=0)=-1$ and $u(x,y,t=0)=-\Delta$, where Δ denotes the dimensionless undercooling, except for the region of the crystal seeds. Inside of crystal seeds, $p(x,y,t=0)=1$ and $u(x,y,t=0)=0$. No-flux boundary conditions are used at $x=0$ and $y=0,L_y$, and fixed boundary conditions $p(x,y)=-1, u(x,y)=-\Delta$ are used at $x=L_x$ in the simulations.

III. SIMULATION RESULTS

A. Tip velocity of doublon

First, we show numerical results for the tip velocity of doublons in an isotropic system, i.e., $e_s=e_k=0$. Two small seeds of crystal of the same size are set on the left side of the channel as an initial condition. Doublons with the mirror-symmetry grow naturally. We have measured the tip velocity, changing the degree of undercooling Δ. We have investigated both cases with and without the kinetic effect. In Fig. 1(a), we show the tip velocity as a function of Δ for the case of no kinetic effect. Figure 1(b) is the same type plot as Fig. 1(a) but the kinetic effect is involved. The plus marks denote the results of numerical simulations, and the solid lines are fitting curves of power laws.

In the theory of Ben Amar and Brener, the tip velocity is proportional to the ninth power of Δ for small Δ [14], although they consider a system of $L_y=\infty$. Kupferman *et al.* showed that an asymmetric dendrite (doublon) cannot exist below a critical undercooling about $\Delta\approx 0.66$. We have observed in our simulations that the groove width between the two fingers is sufficiently small and the effects of the sidewalls seem to be negligible for large Δ. But when Δ is de-

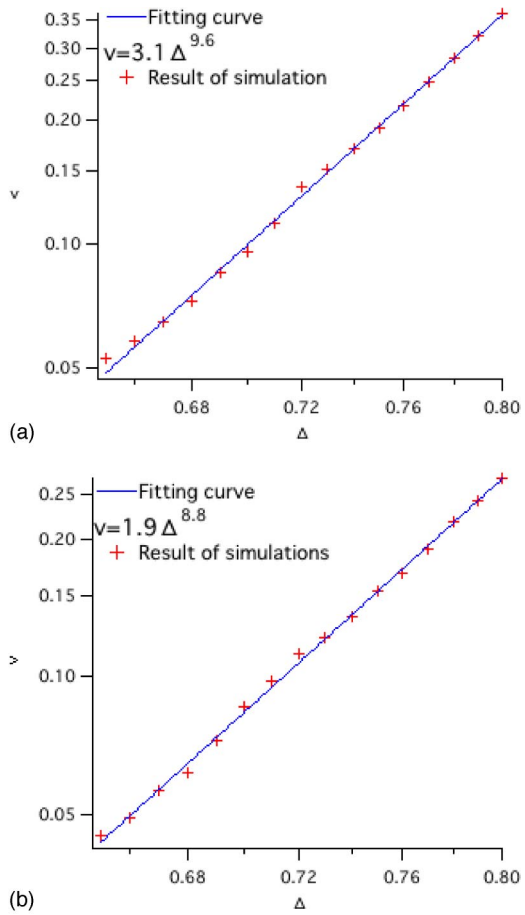

FIG. 1. Double-logarithmic plot of the velocity dependence of the doublon on Δ for (a) $\beta(\theta)=0$ and (b) $\beta(\theta)=d_0\times 0.1=0.03077$.

creased, the tip velocity v becomes very slow and the diffusion length D/v increases up to the order of $L_y/2$ and then the influence of the sidewalls becomes large. If Δ is decreased to 0.64, we cannot regard the growth pattern composed of two fingers as a doublon; it looks like two independent Saffman-Taylor type fingers. So, our results do not contradict to the results of Kupferman *et al.* The numerically estimated exponents of the power law are about 9.6 in case of negligible kinetic effect and 8.8 in case of finite kinetic effect. In both cases, the fitting curves are close to a curve of Δ^9. That is, our result suggests that the tip velocity of doublons satisfies approximately the scaling law found by Ben Amar and Brener, although the undercooling Δ is fairly large and the doublons grow in a channel.

B. Surface tension doublon

In this section, we search for the stable region of doublons in a parameter space of the parameter e_s of the surface tension anisotropy and the undercooling. We judge that a doublon is stable, if a mirror-symmetric doublon is formed as a stable growth structure from an asymmetrical initial condition. To investigate it, we have set two seeds of crystal with different sizes on the left side of the channel as an initial condition. Both of them have a shape of a semicircle. A radius of the one seed is 1.2, and that of the other is 1. The centers of the two seeds locate at $(0,L_y/2-1.6)$ and $(0,L_y/2+1.6)$. In this section, we show the numerical results for the case of no kinetic effect, that is, λ is set to be $(2ID)/(K+JF)$ and $\tau(\theta)=W^2(\theta)$. Since the surface tension anisotropy determines the growth direction, we call this type of doublon a surface tension doublon, as an analogue of the surface tension dendrite. Furthermore, in order to investigate the influence of the sidewalls of channel, we have used two kinds of channels with $L_y=192$ and 96. We have obtained, roughly speaking, similar phase diagrams for the two channels. However, there appeared some patterns which seemed to be strongly influenced by the sidewalls in the simulations of $L_y=96$, so, we show numerical results only for the channel of $L_y=192$. In Fig. 2, we show some time evolutions of patterns. We have judged that the growth patterns are stable doublons if the tip positions for the two fingers approach each other, and confirmed it by the fact that the diffusion length is larger than the width of the groove of the doublon. If the diffusion length is larger than the groove width, two fingers interact with each other via the diffusion field and a bound state of two fingers is formed as a doublon. Figure 2(a) is an example of a stable doublon at $\Delta=0.78$ and $e_s=0.005$. Even if the sizes of two seeds are initially different, a mirror-symmetric doublon is finally generated. In Fig. 2(b) at $\Delta=0.72$ and $e_s=0.02$, two fingers are generated but one finger overcomes the other. The difference of the tip positions of two fingers increases in time. The doublon is not formed at this parameter set. In Fig. 2(c) at $\Delta=0.82$ and $e_s=0.01$, the groove is partially buried, although the tip structure keeps a stable one. This type of growth pattern appears in the range of high undercooling. In our phase-field model, the interface between the solid and the liquid has a finite thickness. On the other hand, the groove becomes narrower as the undercooling is increased. We expect that the partial disappearance of the groove occurs when the interface thickness becomes comparable to the groove width, so this may be an artifact of the phase-field model. In Fig. 2(d) at $\Delta=0.62$ and $e_s=0.005$, the growth directions of the two fingers are declined from the x direction, since the anisotropy parameter e_s is very small, and the two fingers grow like the Saffman-Taylor fingers with very small velocities. This is a typical pattern, which appears in the range of low undercooling. The tip velocity is very small because of the low undercooling. Since the diffusion length D/v is sufficiently large and it is comparable to or larger than $L_y/2$, the interaction with the sidewalls becomes important. If the sidewall effects are absent, a stable doublon may appear, but we could not judge it a stable doublon in our channel of $L_y=192$ at the parameters $\Delta=0.62$ and $e_s=0.005$. Kupferman *et al.* also showed that the doublon cannot exist for $\Delta<0.66$ for $e_s=0.006$. A more drastic example, where a doublon could not be formed, is displayed in Fig. 2(f) at $\Delta=0.72$ and $e_s=0.04$. The competitive time evolution of two fingers is not seen at all, and a single dendrite appears from the beginning. In a fairly large parameter region, we have found doublons, whose grooves are slightly oscillating, although the oscillation gradually attenuates and stationary doublons are finally obtained in most cases. Figure 2(e) displays a doublon

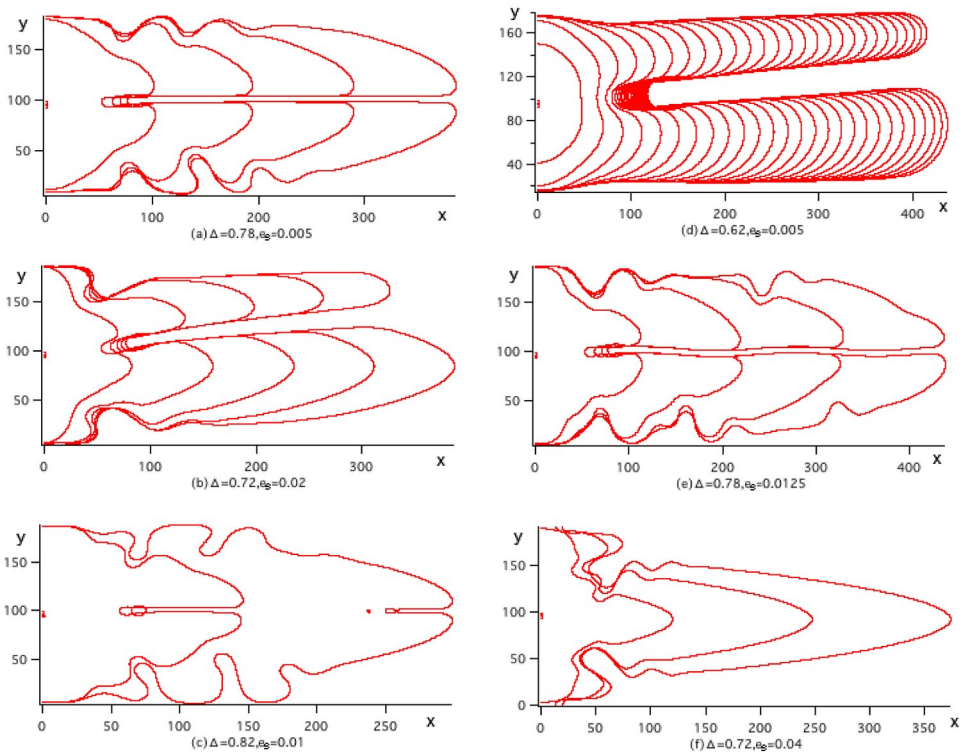

FIG. 2. Several growth patterns for surface tension doublons. (a) Stable doublon made by surface anisotropy. (b) One finger wins. (c) Surface tension doublon whose groove is partially buried. (d) Two fingers pattern of surface tension doublon. (e) Oscillating groove. (f) A surface tension dendrite.

accompanying such damping groove oscillation. In a very narrow parameter range around (g) in Fig. 3, the groove oscillation does not decay and the limit cycle of groove oscillation is observed. We study the groove oscillation more in detail in Sec. IV B.

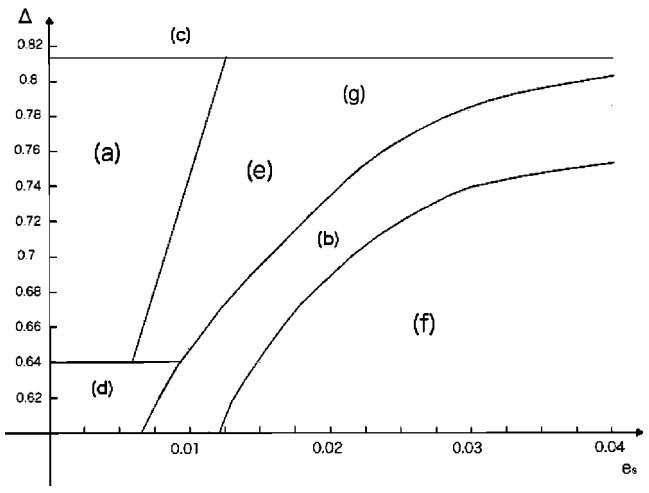

FIG. 3. Phase diagram of surface tension doublon. The alphabets in the figure correspond to the growth patterns in Fig. 2. The region around (a) is a parameter region where a stable doublon has appeared. In the region around (e), the doublons with an oscillating groove appear. The doublon structure has not been formed in the region around (b), (d) and (f). The region around (c) denotes a region where the doublonlike pattern is stable; however, the groove is partially buried. In a very narrow parameter range around (g), the groove oscillation does not decay and the limit cycle of groove oscillation is observed.

In Fig. 3, we show a phase diagram for the stability of doublons. This phase diagram was obtained by changing Δ stepwise by 0.02 from 0.6 to 0.82 and e_s by 0.0025 from 0 to 0.04, and the transition lines were drawn smoothly by hands. This phase diagram was drawn by observing the time evolutions of growth patterns for each parameter set (e_s, Δ) using the same initial condition used for the simulations shown in Fig. 2. The alphabets in the figure correspond to the patterns shown in Fig. 2. In the regions (a), (c) and (e), stable doublons have appeared. The doublons are stationary in the region (a), the groove oscillation is seen in a parameter region around (e), and the groove is partially buried in the region (c) (although it may be an artifact of the phase-field model). In the regions (b), (d) and (f), stable doublons have not been formed. A single dendrite has appeared from the beginning in the region (f), competitive time evolution of two fingers is observed in the region (b) and the formation of doublons is not observed probably owing to the finiteness of L_y in the region (d). In general, high undercooling and low anisotropy are favorable for the formation of doublons. If the surface tension anisotropy increases too much, a doublon cannot be formed, instead, a stable dendrite appears. As the undercooling is decreased too much for relatively small e_s, a doublon cannot be formed, instead, two independent Saffman-Taylor-like fingers appear. We have drawn a phase diagram in Fig. 3 using only one initial condition. The competitive time evolution between two fingers depends on the initial conditions and the computation time (for example, if the size difference of the initial two seeds is very small, it takes very long time for the competitive dynamics), and therefore the boundary line between stable doublons (a), (c), (e) and dendrites (b), (f) in Fig. 3 is expected to depend on the initial conditions. (See the discussion in Sec. IV.) It is expected that there is no

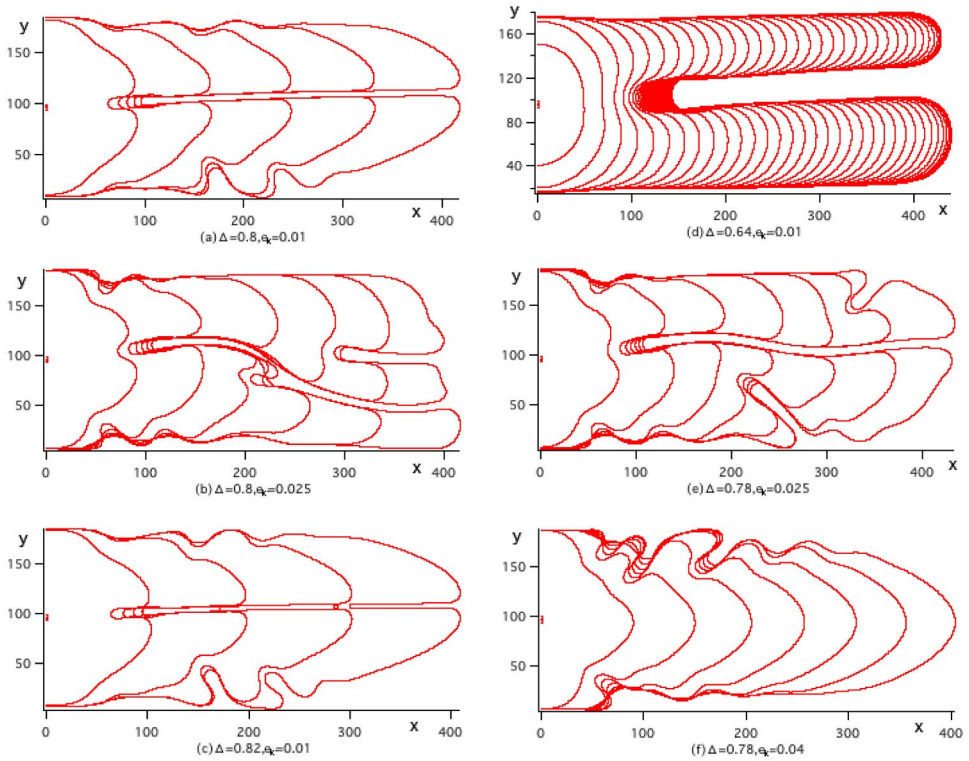

FIG. 4. Several growth patterns for kinetic doublons. (a) Stable doublon made by kinetic anisotropy. (b) Tip splitting. (c) Kinetic doublon whose groove is partially buried. (d) Two finger pattern of kinetic doublon. (e) Oscillating groove. (f) A kinetic dendrite.

boundary between stable doublons (a), (c), (e) and two Saffman-Taylor type fingers (d) if the width L_y is infinity, since doublons exist stably even at $e_s=0$ for $L_y=\infty$.

C. Kinetic doublon

Next, we show the results of numerical simulations including the kinetic effect. For simplicity, the surface tension anisotropy is assumed to be 0, i.e., $e_s=0$. The initial conditions are the same as in Sec. III B. The growth direction is determined by the kinetic anisotropy, and we call this type of doublon a kinetic doublon in this paper as an analogue of the kinetic dendrite. If the kinetic parameter e_k takes a negative value, patterns grow along the channel direction. For the sake of simplicity, we express the absolute value of e_k as e_k hereafter. In Fig. 4, we show typical growth patterns of kinetic doublons. Figure 4(a) shows a stable doublon pattern at $\Delta=0.8$ and $e_k=0.01$. In Fig. 4(b), a stable doublon cannot be formed and tip splittings occur at $\Delta=0.8$ and $e_k=0.025$. Figure 4(c) displays a doublonlike pattern at $\Delta=0.82$ and $e_k=0.01$, where the groove is partially buried owing to too large undercooling. Figure 4(d) is a pattern at $\Delta=0.64$ and $e_k=0.01$. The tip velocity is very slow and the diffusion length is sufficiently large. The doublon cannot be formed and two Saffman-Taylor-like fingers appear owing to too low undercooling and relatively small anisotropy. Figure 4(e) is interpreted as a doublon with groove oscillation at $\Delta=0.78$ and $e_k=0.025$. Figure 4(f) shows a pattern at $\Delta=0.78$ and $e_k=0.04$, in which only one finger appears from the beginning and it grows into a kinetic dendrite. Figure 5 is a phase diagram for the stability of the kinetic doublon. The alphabets in the figure correspond to the patterns shown in Fig. 4. In the regions (a) and (c), stable doublons are observed. In the region (f), a single kinetic dendrite appears from the beginning. In the region (d), the tip velocity is too slow, stable doublons are not formed, and two fingers like the Saffman-Taylor fingers appear. In the transition regions around (b) and (e), complicated patterns appear. In the region around (b), tip-splitting are observed, and in the region around (e), the

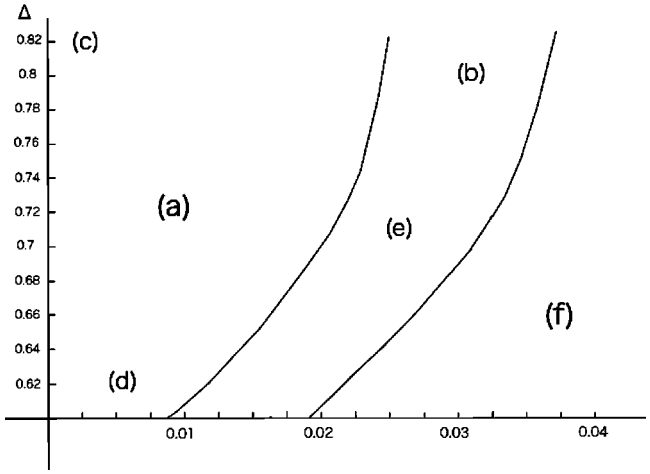

FIG. 5. Phase diagram of kinetic doublon. The alphabets in the figure correspond to the patterns in Fig. 4. In the region around (a), the stable doublon has appeared. In the region around (e), a groove of the doublon exhibits damping oscillation or tip branching. We can find tip splitting patterns in the region around (b). In the region around (d) and (f), a stable doublon has not been formed. In the region around (c), a pattern with partially buried groove has appeared.

groove oscillation is observed. The difference of the two phase diagrams shown in Figs. 3 and 5 for the surface tension doublon and kinetic doublon is discussed in Sec. V.

IV. TRANSITIONS OF DOUBLONS

A. Transitions between doublons and dendrites

In the previous section, we have shown phase diagrams for the surface tension doublon and the kinetic doublon. When the anisotropy is weak and the undercooling Δ is large, stable doublons have been observed. It is known that the dendrite is linearly (or marginally) stable if the anisotropy parameter is not zero and $L_y=\infty$ [2,3,7]. The doublon and the dendrite can therefore coexist in a certain parameter range. That is, which structure appears depends on the initial conditions. The transitions between the dendrites and the doublons in a channel were studied in detail by Kupferman *et al.* [21]. They showed that the transition from symmetric dendrites to parity-broken dendrites (doublon) is continuous for $e_s=0$ and 0.006 but it is discontinuous and the velocity jumps at $e_s=0.00667$. They also showed that both the doublon and the dendrite are linearly stable for a certain parameter region. Ben Amar and Brener discussed the transition between the dendrite and the doublon for a system of $L_y=\infty$, and expected that there is a velocity jump at the transition. The width of our channel is slightly wider and our anisotropy parameter is larger in most cases than the case of Kupferman *et al.*, so the effects of the sidewalls seem to be weaker than the case of them. We will investigate whether such a velocity jump exists in our system. To investigate it, we change the anisotropy parameters slowly stepwise, since there is hysteresis generally in bistable systems and which pattern appears depends on the initial conditions. Our numerical procedure is as follows. Two small seeds of crystal with the same size are set on the left side of the channel as an initial condition for the doublonlike pattern at a certain small anisotropy parameter (for example $e_s=0.01$), and a single small seed of crystal is set in the middle of the left side of the channel as another initial condition for the dendritic pattern at a large anisotropy parameter (for example $e_s=0.06$). If the tip of the growth pattern reaches a critical value (for example, $x=x_c=440$) in a box of $L_x\times L_y=480\times 200$ for a certain anisotropy parameter, the time evolution is stopped, and the numerical data for the order parameter and the temperature are saved in computer. The order parameter and the temperature profiles in the tip region $[p'(x,y),u'(x,y)]$ are used as the initial condition for the next anisotropy parameter as $p(x,y,t=0)=p'(x+340,y)$, and $u(x,y,t=0)=u'(x+340,y)$. (For example, e_s is increased by 0.01 for doublonlike patterns, and e_s is decreased by 0.01 for dendritic patterns.) We have repeated the above processes by changing the anisotropy parameter stepwise. Both doublonlike patterns and dendritic patterns keep the mirror-symmetric forms in this time evolution even if the anisotropy parameters are changed. We have calculated the tip velocities for doublonlike patterns and dendritic patterns. Figure 6 displays the tip velocities of surface tension doublons and surface tension dendrites for $0.01\leqslant e_s\leqslant 0.06$ for a fixed value of undercooling $\Delta=0.75$. The tip velocities of the doublons are always larger than the dendrites, but the velocity difference changes continuously and becomes almost 0 at $e_s=0.04$. We could not find a clear jump of velocity difference predicted by Ben Amar and Brener [14] in this simulation. The continuous transition may be consistent with the results of Kupferman *et al.* for small anisotropy. Cooperative interaction between the two fingers makes the tip velocity of doublons faster than that of dendrites. Since the two types of patterns have almost the same velocity for $e_s>0.04$, doublonlike patterns with two fingers may be interpreted as patterns composed of two independent dendrites. The parameter $e_s=0.04$ can be interpreted as a transition point from doublons to dendrites for $\Delta=0.75$. We have investigated the stability of doublonlike patterns by dislocating initially the two fingers of the doublonlike patterns. That is, the initial condition was slightly changed as $p(x,y,t=0)=p'(x+340,y)$, $u(x,y,t=0)=u'(x+340,y)$ for $x<140$ and $y>100=L_y/2$ and $p(x,y,t=0)=p'(x+344,y)$, $u(x,y,t=0)=u'(x+344,y)$ for $x<140$ and $y<100=L_y/2$, where $p'(x,y)$ and $u'(x,y)$ are the saved data of the mirror-symmetric doublon. That is, the lower half of the doublon is shifted by 4 in the direction of x. The difference of the tip positions of the two fingers is therefore 4 initially. We have investigated the time evolution of the difference of the tip positions. Figure 7 displays the time evolutions for four parameters $e_s=0.06$, 0.04, 0.02, and 0.01. The difference ΔX_p of the tip positions increases monoto-

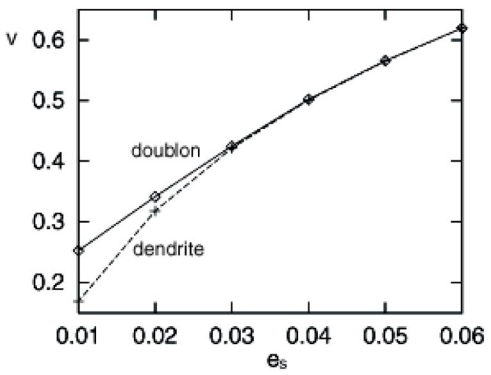

FIG. 6. Tip velocities of doublonlike patterns (solid curve) and dendritic patterns (dashed curve) as a function of e_s for $\Delta=0.75$.

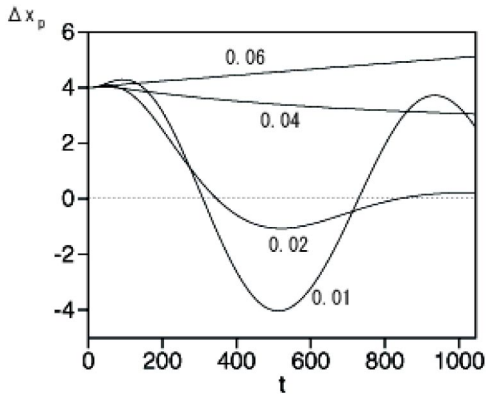

FIG. 7. Time evolutions for the difference of the tip positions for four parameter values $e_s=0.06$, 0.04, 0.02, and 0.01.

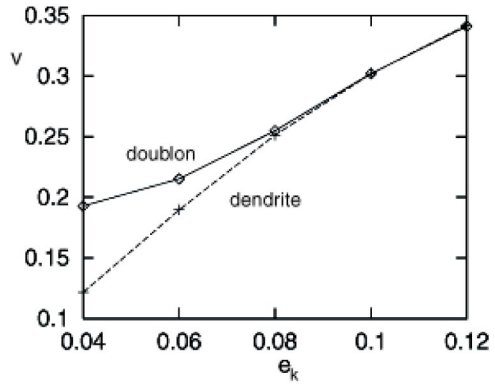

FIG. 8. Tip velocities of kinetic doublons (solid curve) and kinetic dendrites (dashed curve) as a function of e_k for $\Delta = 0.78$.

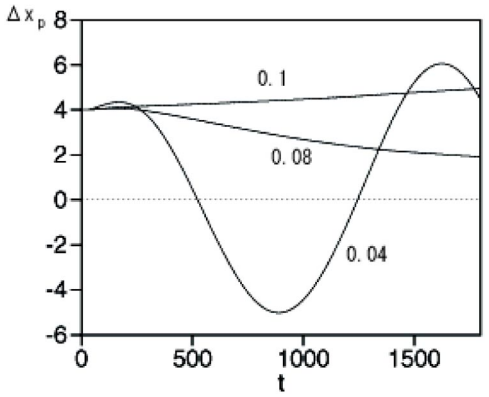

FIG. 9. Time evolutions for the difference of the tip positions for three parameter values $e_k = 0.04$, 0.08, and 0.1.

nously for $e_s = 0.06$. The leading finger overcomes the other after a long run at this parameter. This corresponds to the competitive time evolution of two fingers, as seen in the previous section. At $e_s = 0.05$, the difference ΔX_p increases very slowly, but it decays monotonously for $e_s = 0.04$ and 0.03. It means that the doublon structure with the mirror symmetry is recovered for $e_s \leqslant 0.04$ after a long run, that is, the doublon structure is stable. This critical parameter $e_s \approx 0.045$ is almost the same as the transition parameter where the difference between the tip velocities of the doublon and the dendrite becomes 0. This transition point is rather larger than the transition point $e_s \approx 0.023$ found in Fig. 3. This is not a contradiction since the transition curve in Fig. 3 is determined by numerical simulations starting from a certain initial condition. This critical parameter $e_s \approx 0.045$ is expected to be obtained when the initial size difference of the two seeds is infinitesimally small. The difference ΔX_p exhibits damping oscillation for $e_s = 0.01$ and 0.02. This corresponds to the groove oscillation in the previous section. The groove oscillation occurs below another critical parameter $e_s \approx 0.025$, which is smaller than the critical parameter $e_s \approx 0.045$ for the stability of doublons. That is, the oscillatory behavior appears inside the stable region of doublons. The transitions between the doublons and the dendrites studied by Kupferman *et al.* in a channel are very complicated for nonzero e_s, and the oscillatory behaviors are not reported in their paper [21]. The detailed quantitative comparison with their results is left to future study.

We have performed the same type simulations to study the transition between kinetic doublons and kinetic dendrites. The undercooling was fixed to be 0.78, and the kinetic anisotropy e_k was changed from 0.04 to 0.12. The parameter λ was fixed to be $1.6ID/(K+JF)$, i.e., $\beta(\theta) \propto 0.2 + e_k \cos 4\theta$. (The parameter value of λ is slightly different from that used in Sec. III C.) Figure 8 displays the tip velocities of doublons and dendrites. The tip velocities of doublons are always larger than dendrites. As e_k is increased, the difference of the tip velocities for the two patterns is decreased and becomes almost 0 for $e_k \geqslant 0.1$. The doublonlike patterns cannot be distinguished from two independent dendrites for $e_k \geqslant 0.1$ similarly to the case of the surface tension doublons. We have also investigated the time evolution of the tip positions of the two fingers by dislocating the two fingers of an originally mirror-symmetric doublon, just as the case of the surface tension doublons for $e_k = 0.04$, 0.06, 0.08, 0.1 and 0.12. Figure 9 displays the time evolutions of the difference of the tip positions for three parameters $e_k = 0.04$, 0.08 and 0.1. The difference of the tip positions increases monotonously for $e_k = 0.12$ and 0.1. It suggests that the leading finger wins the other and a single dendrite will survive after a long run. This again corresponds to the competitive time evolution of the two fingers. For $e_k = 0.08$, the tip difference decays monotonously. The critical value $e_k \approx 0.09$ is almost the same as the parameter where the difference of the tip velocities of the doublon and the dendrite becomes zero, as the case of the surface tension doublon. The time evolution of ΔX_p exhibits damping oscillation for $e_k = 0.06$. The oscillatory behaviors appear below another critical value different from the first critical value $e_k \approx 0.09$. For $e_k = 0.04$, the oscillation seems to grow in time. We have continued the calculation for $e_k = 0.04$, and found that the amplitude of the oscillation becomes too large and the two fingers are too separate and seem to become almost independent after a long run.

B. Groove oscillation of doublons

As shown in Secs. III and IV A, there is a fairly large parameter region, where the grooves of doublons exhibit oscillation. In most cases, the oscillation decays in time and a steadily growing doublon is obtained after a long run. We have found that the oscillation does not decay in time in a very narrow parameter region for the surface tension doublon. Figure 10 shows a doublon with the limit cycle of groove oscillation at $\Delta = 0.8$ and $e_s = 0.021$. A longer channel of $L_x \times L_y = 1300 \times 192$ is used in this simulation to show that the groove oscillation does not decay. Figures 11(a) and 11(b) display the time evolutions of the difference ΔX_p of the tip positions of the two fingers for $e_s = 0.021$ (a) and 0.022 (b) at $\Delta = 0.8$. It is clearly seen that the groove oscillation is sustained at $e_s = 0.021$, but the oscillation decays in time at $e_s = 0.022$. Figure 12 displays the root mean square of the tip oscillation $\sqrt{(\Delta X_p)^2}$ as a function of e_s for $\Delta = 0.8$. The groove oscillation appears for $0.018 \leqslant e_s \leqslant 0.021$, and the transition seems to be a subcritical one, since there is a jump of the oscillation amplitude. We have performed a few simulations with a wider system of $L_y = 384$ to confirm the sta-

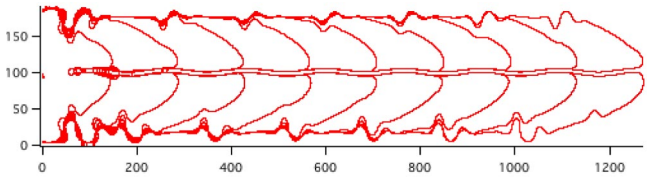

FIG. 10. A doublon with the limit cycle of groove oscillation at $\Delta = 0.8$ and $e_s = 0.021$.

bility of the groove oscillation. We observed the groove oscillation with the same amplitude also in this wider system. It implies that the groove oscillation is not due to the effect of the sidewalls. The competitive interaction between the two fingers in a single doublon is the origin of the groove oscillation. Similar type of oscillation was observed in numerical simulations of directional solidification by Losert *et al.* [16]. In their simulations, the spacing of the doublet cellular array exhibits vascillation, and the grooves between the cells oscillate accompanying the vascillation, when the spacing of the cellular array is too smaller. The interaction among neighboring doublet cells seems to be important in the simulations of Losert *et al.* In our system, the groove oscillation occurs in a single doublon, and the effects of the sidewalls are negligible. We do not understand well the mechanism of the groove oscillation yet, but the mechanism seems to be different from the case for the directional solidification studied by Losert *et al.*

V. DISCUSSION

We have performed numerical simulations of doublons with the phase-field model to obtain phase diagrams for the

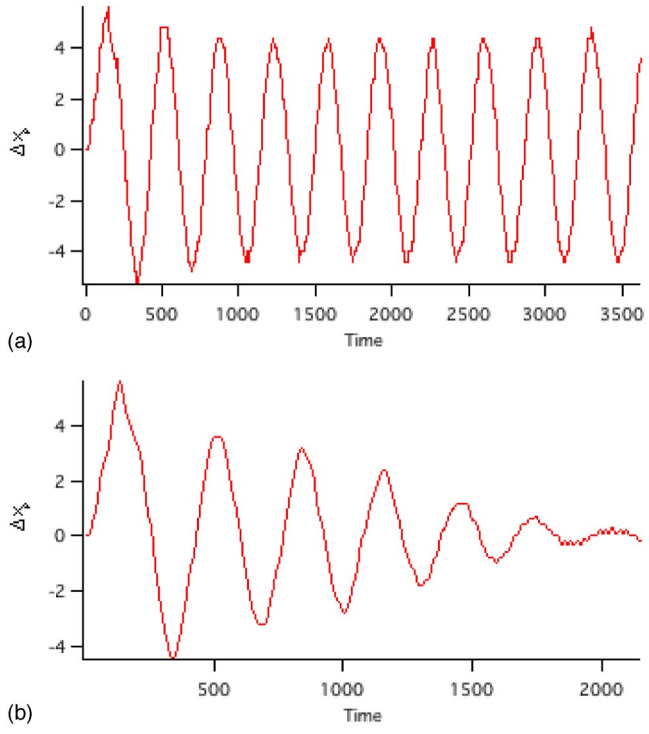

FIG. 11. The time evolutions of the difference ΔX_p of the tip positions of the two fingers for $e_s = 0.021$ (a) and 0.022 (b) at $\Delta = 0.8$.

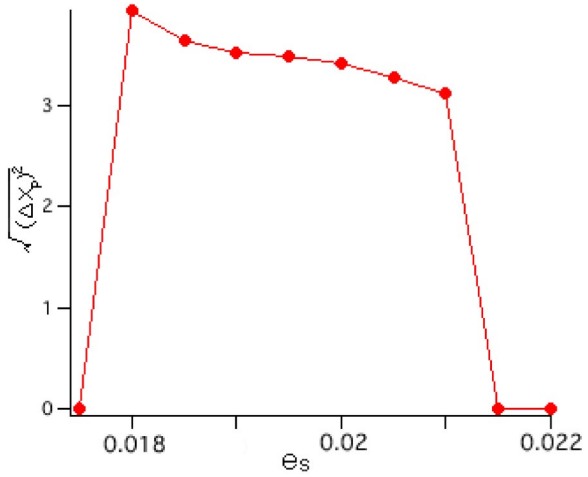

FIG. 12. The root mean square of the oscillation $\sqrt{(\Delta X_p)^2}$ as a function of e_s for $\Delta = 0.8$.

stability of doublons. A doublon can be interpreted as a stable bound state of two fingers. When the anisotropy is sufficiently weak and L_y is large, a single finger is unstable and tip-splittings will occur. If the two unstable fingers interact with each other and form a doublon, the bound state is stabilized and grows faster than a single finger. We will add some qualitative explanations for our numerical results in this section.

Figure 1 shows that the tip velocities of doublons involving kinetic effect are smaller than doublons without kinetic effect for the same values of Δ. This is because the kinetic effect decreases the interface temperature u_i owing to Eq. (6) and therefore the effective undercooling at the interface is decreased. This leads to the smaller power of the fitting curve in Fig. 1(b) for the kinetic doublons. However, in the range of the very small Δ, it is predicted that the tip velocity does not depend on the kinetic effect, since the tip velocity is sufficiently small for the range of very small Δ and the second term in the right-hand side of Eq. (6) could be negligible. But, the scaling law will not be satisfied for small Δ in a channel system, since the doublons will become two independent Saffman-Taylor-like fingers as suggested by Kupferman *et al.* To find the deviation more clearly, it is desirable to study the tip velocity for even smaller Δ.

The groove of the doublon is partially buried in a parameter region of large undercooling. It is probably because the width of the groove becomes narrower as Δ increases. When the width of the groove becomes the same order as the width of the interface of the order parameter, the groove shrinks and partially disappears. This may be an artifact of the phase-field model.

We have found that stable doublons are formed in a parameter region of high undercooling and low anisotropy. This result is consistent with the previous predictions [18,19], in which qualitative phase diagrams for the stable region of doublons were given. We have obtained phase diagrams more quantitatively using the phase-field model. The doublon cannot be formed in a strongly anisotropic system, instead, a dendrite appears as a stable growth pattern. Ben Amar and Brener predicted that the doublon appears in a

parameter region satisfying $\Delta > e_s^{1/4}$ and there is a jump of the velocity difference between the doublon and the dendrite for the system $L_y = \infty$. Kupferman *et al.* showed that the transition from the dendrite to the doublon is continuous and there is no velocity jump in a narrow channel for small e_s [21]. Our simulations were performed in a channel, where the width is slightly wider than the case studied by Kupferman, but the surface tension anisotropy is generally stronger than the case of Kupferman *et al.* We could not find the velocity jump and our result is consistent with the result by Kupferman *et al.* for small e_s. If the criterion for the transition from doublon to dendrite is that the velocity difference becomes 0 as is suggested in Sec. IV, the transition curve may be roughly evaluated as $\Delta \propto e_s^{7/20}$, since the velocity $v \propto \Delta^9$ for doublons is equal to the velocity $v \propto e_s^{7/4}\Delta^4$ of the dendrite at the transition curve. We have also found that kinetic doublons cannot be formed when the anisotropy is large and the undercooling is small. Near the transition points, the tip velocities of doublons and dendrites are almost the same. If the difference of the two tip velocities becomes 0 at the transition curve from the doublon to the dendrite, the transition curve may be evaluated even for the kinetic doublons as follows. The velocity of doublon is estimated as $v \propto \Delta^9$. Brener and Melnikov studied dendrites involving strong kinetic effect based on the solvability theory [3]. The tip velocity of the kinetic dendrite is estimated as $v \propto e_k^{5/4}\Delta^2$ for $e_s = 0$. If the velocity of the kinetic dendrite is equal to that of doublon, the transition curve between kinetic doublons and kinetic dendrites is evaluated as $\Delta \propto e_k^{5/28}$. This exponent 5/28 is smaller than the exponent 7/20 for the surface tension doublon. We have not yet identified these exponents in phase diagrams of Figs. 3 and 5. The phase diagrams in Figs. 3 and 5 were obtained using only a specific initial condition and the resolution of the phase diagrams is rather rough. In the derivation of the exponents, the sidewall effects are neglected and the velocity scalings for doublons and dendrites are applicable for small undercooling, therefore, it is questionable that the theoretical values of the exponents can be applied in our channel system for relatively large Δ. It is left to future study to obtain more elaborate phase diagrams with different initial conditions such as the one used in Sec. IV A and algorithms of higher performance [22] and evaluate quantitatively the boundary curves between doublons and dendrites.

The most interesting growth form is the oscillating doublon. The difference of the tip positions of the two fingers exhibits clear oscillation as shown in Figs. 7, 9, and 11. It implies that one finger which has fallen behind the other once, catches up with and then passes through the other finger after a while. The oscillation decays in time in most cases, but does not seem to decay in a very narrow parameter region as shown in Figs. 10–12. The groove oscillation of doublons is observed in a parameter region inside of the stable region of doublons, that is, the boundary curve for the oscillatory behavior is apart from the transition curve between doublons and dendrites, as is discussed in Sec. IV A. In a previous paper, we found tip oscillation of doublons and periodic side-branchings in a different parameter region, where the surface tension anisotropy and the kinetic anisotropy compete, with the phase-field model in a channel [13]. The groove oscillation and the tip oscillation are two different modes of oscillation for a doublon.

[1] J. S. Langer, Rev. Mod. Phys. **52**, 1 (1980).
[2] Y. Saito, *Statistical Physics of Crystal Growth* (World Scientific, Singapore, 1996).
[3] E. A. Brener and V. I. Melnikov, Adv. Phys. **40**, 53 (1991).
[4] S. K. Chan, H. H. Reimer, and M. Kahlweit, J. Cryst. Growth **32**, 303 (1976).
[5] S. C. Huang and M. E. Glicksman, Acta Metall. **29**, 714 (1981).
[6] A. Dougherty, P. D. Kaplan, and J. P. Gollub, Phys. Rev. Lett. **58**, 1652 (1987).
[7] D. A. Kessler, J. Koplik, and H. Levine, Phys. Rev. A **33**, 3352 (1986).
[8] Y. Saito, G. Goldbeck-Wood, and H. Müller-Krumbhaar, Phys. Rev. Lett. **58**, 1541 (1987).
[9] H. Sakaguchi and M. Ohtaki, Physica A **272**, 300 (1999).
[10] R. Kobayashi, Physica D **63**, 410 (1993).
[11] A. Karma and W. J. Rappel, Phys. Rev. E **53**, 3017 (1996).
[12] A. Karma and W. J. Rappel, Phys. Rev. E **57**, 4323 (1998).
[13] H. Sakaguchi and S. Tokunaga, Prog. Theor. Phys. **110**, 1043 (2003).
[14] M. Ben Amar and E. Brener, Phys. Rev. Lett. **75**, 561 (1995); Physica D **98**, 128 (1996).
[15] H. Jamgotchian, R. Trivedi, and B. Billia, Phys. Rev. E **47**, 4313 (1993); S. Akamatsu, G. Faivre, and T. Ihle, *ibid.* **51**, 4751 (1995).
[16] P. Kopczynski, W.-J. Rappel, and A. Karma, Phys. Rev. E **55**, R1282 (1997); W. Losert, D. A. Stillman, H. Z. Cummins, P. Kopczynski, W.-J. Rappel, and A. Karma, *ibid.* **58**, 7492 (1998).
[17] N. Samid-Merzel, S. G. Lipson, and D. S. Tannhauser, Physica A **257**, 413 (1998).
[18] T. Ihle and H. Müller-Krumbhaar, Phys. Rev. Lett. **70**, 3083 (1993); Phys. Rev. E **49**, 2972 (1994).
[19] E. Brener, H. Müller-Krumbhaar, and D. Temkin, Phys. Rev. E **54**, 2714 (1996).
[20] E. Brener, H. Müller-Krumbhaar, Y. Saito, and D. Temkin, Phys. Rev. E **47**, 1151 (1993).
[21] R. Kupferman, D. A. Kessler, and E. Ben-Jacob, Physica A **213**, 451 (1995).
[22] M. Sabouri-Ghomi, N. Provatas, and M. Grant, Phys. Rev. Lett. **86**, 5084 (2001).